Modern Physics Letters B
Vol. 37, No. 15 (2023) 2350046 (10 pages)

DOI: 10.1142/S021798492350046X

World Scientific
www.worldscientific.com

Nickel oxide nanoparticles: Synthesis and characterization for optical studies

B. Shanmugapriya*, G. Sivasankari†, K. Kannagi*,‖, P. Sankari‡, R. A. Kiruthika*, N. Pavithra*, Asla A. Al-Zaharani§ and Mahanim Sarif¶

*PG & Research Department of Physics, Cauvery College for Women (Autonomous), Affiliated to Bharathidasan University, Trichy 620018, Tamil Nadu, India

†PG & Research Department of Chemistry, Cauvery College for Women (Autonomous), Affiliated to Bharathidasan University, Trichy 620018, Tamil Nadu, India

‡MIT College of Arts & Science, Musiri, Affiliated to Bharathidasan University, Trichy 621211, Tamil Nadu, India

§Department of Chemistry, Science College, Imam Abdulrahman Bin Faisal University, Dammam 34212, Saudi Arabia

¶Bioenergy Branch, Forest Research Institute Malaysia (FRIM), 52109, Malaysia

‖kannagi.natraj@gmail.com

Received 24 November 2022
Revised 10 February 2023
Accepted 21 February 2023
Published 27 April 2023

In this study, the co-precipitation approach was used to make nanostructured nickel oxide (NiO) commencing with sodium hydroxide (NaOH) and nickel (II) chloride hexahydrate (NiCl2·6H2O). Through the use of X-ray diffraction (XRD), scanning electron microscopes (SEM), UV-visible (UV–Vis) absorption, and Fourier transform infrared (FTIR) imaging, structural and optical studies were investigated. FTIR, photoluminescence (PL), cyclic voltammetry (CV) studies are taken. The synthesized nanoparticles were annealed at 300°C and 400°C. The face-centered cubic (FCC) structure of the NiO and highly crystallized nanoparticles were revealed by XRD investigations. Observation of FTIR spectra validated the composition of functional groups. Scanning electron microscopy image shows the average size is 24 nm. NiO optical band gap at 300°C

‖Corresponding author.

(3.37 eV) and 400°C (2.7 eV) is revealed from UV studies. From CV graph, the sample annealing at 300°C and 400°C the specific capacitance was 543.6 and 519.8 F/g, respectively. This study signifies the supercapacitor application of nanosized metal oxide.

Keywords: Co-precipitation; NiO; morphology; nanoparticles; CV and supercapacitor.

1. Introduction

Both nanoscience and nanotechnology are built on the foundation of nanomaterials. The study of nanostructures is a vast, interdisciplinary topic of research and growth that has gained enormous global attention in recent years. Nanoparticles and man-made materials are being generated in large quantities all around the world at an accelerated rate.[1,2] They have the ability to change the types and range of functions that are available, as well as how products and materials are manufactured. Due to their numerous uses, nanomaterials are becoming more and more ingrained in our daily lives. However, a major cause of concern is their detrimental impact on both the environment and human life.[3] It will surely have a significant business influence, which will only grow in the future. A class of materials with at least one dimension smaller than 100 nanometers are referred to as "nanostructured materials." A nanometer is one-millionth of a millimeter, 100,000 times lower than the width of a human hair. Because they have unusual optical, electromagnetic, electronic and other qualities at such a small scale, nanomaterials are fascinating. These new characteristics could have a significant impact on electronics, health, as well as other fields. Irresolvable metal oxide nanoparticles are anticipated to be more environment-friendly and persistent in terms of bioaccumulation and toxicity; research into these types of properties helps to evaluate potential risks and gives industry information for creating safer nanomaterials.[4–6] Due to its distinct functional characteristics and significance in a broad range of technical applications, nickel oxide (NiO) is being investigated as an electrical device, ceramic material, and catalyst. Overall, NiO is thought to be less hazardous than other nickel compounds.[7–10] Numerous mechanical and chemical techniques have been used to produce NiO nanoparticles of nanoscale dimensions. For many of them, creating materials for technological applications and reducing the cost of chemical synthesis are the major goals. The produced nanoparticles were annealed at 300°C and 400°C and were characterized using X-ray diffraction (XRD), Fourier transform infrared spectroscopy (FTIR), UV-visible (UV–Vis) spectroscopy, photoluminescence (PL) examinations, and electrochemical experiments. The NiO nanoparticles behave like supercapacitors. This research aims to produce NiO nanoparticles using the simple and inexpensive co-precipitation process with sodium hydroxide (NaOH), which only needs a little number of initial materials. The unique aspect of the work is that we carefully examined the structural and optical characteristics of NiO nanoparticles. NiO has been used as a catalyst, an electrode material, a magnetic material, an electrochromic display material and a functional layer material for chemical sensors.[1]

The interest in nanoscale materials has increased along with developments in all fields of business and technology. This is due to the need for novel qualities at this nanoscale as well as the fact that these properties vary with size and morphology.[11]

2. Experimental Procedures

2.1. *Synthesis of NiO nanoparticles*

By utilizing $NiCl_2 \cdot 6H2O$ and NaOH as raw material, double-distilled water was used as the dispersing solvent to create Nio nanoparticles. To achieve a specific molarity at room temperature, 5.9412 g of $NiCl_2 \cdot 66H2O$ was first dissolved in 250 CC of double-distilled water. The resulting solution was then agitated magnetically for 40 minutes at a temperature of 50°C. Then, until the pH was 8, 10 CC of NaOH with a certain molar was gradually added to the solution. The synthesized nanoparticle was cleaned using distilled water to remove any reaction byproducts and then dried for 14 h at 80°C. Then, samples were dried and oxidized (annealed) for 2 h at 300°C and 400°C to produce NiO nanoparticles. This annellation causes the sample's color to transition from greenish to black.

3. Result and Discussion

3.1. *Structural studies XRD*

The observed powdered XRD pattern shown in Fig. 1 corresponds to the NiO nanoparticles and two different samples annealed at 300°C, 400°C intensity of peaks

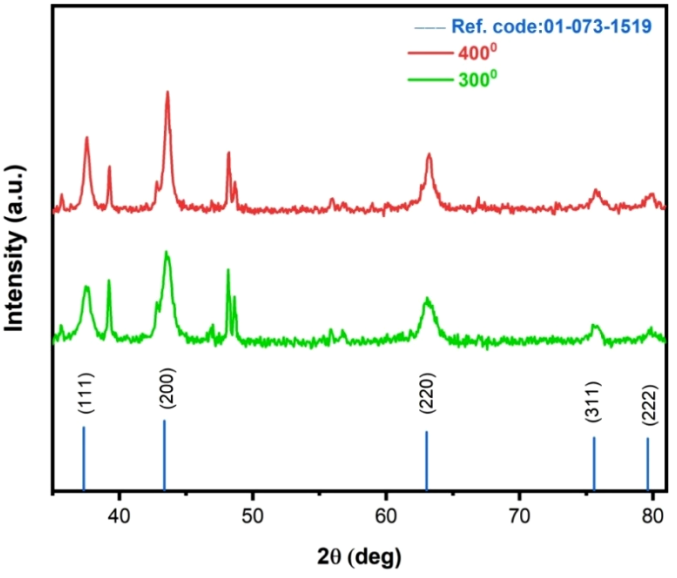

Fig. 1. (Color online) Powder XRD pattern.

increased represents the increase in the sample's crystallinity.[8,12] Sharp diffraction peaks were generated by raising the annealing temperature to 400°C while comparing the peaks at 300°C. The crystalline size may be more or less equal.[12] Five sharp and strong Bragg peaks are observed with their maxima centered at 2θ — 37.60, 43.60, 63.20, 75.80,79.80 corresponding to (111), (200), (220), (311), (222) plane of the cubic structure having $Fm3/m$[10] space group (JCPDS Ref. code: 01-073-1519).[13] The XRD pattern of the synthesized NiO nanoparticles. In addition to the broad Bragg peaks, which belong to the face-centered cubic (FCC) NiO, there is a series of sharp peaks which are not characteristic of NiO, they may be related to traces of non-decomposed $NiCl_2$. The following Scherrer's formula[13–15] was employed to determine crystallite size:

$$D = \frac{k\lambda}{\beta \cos n\theta}, \tag{1}$$

where λ stands for the radiation's wavelength (1.54056 for Cu–K radiation), k for a constant of 0.94, for the peak's breadth at half-maximum intensity and the peak position. Crystallite size for the sample annealed at 300°C and 400°C was 12.9632 and 12.9634 nm. Almost nanoparticles of the same crystallite size were found, which was observed in further calculations. The following formula was used to determine microstrain

$$\varepsilon = \frac{\beta \cos \theta}{4}. \tag{2}$$

For both samples, almost same microstrain was calculated as 0.1558. From the Williamson and Smallman's formula,

$$\delta = \frac{1}{D^2}. \tag{3}$$

Dislocation density was found to be 5.95×10^{-3} (lines/m^2).

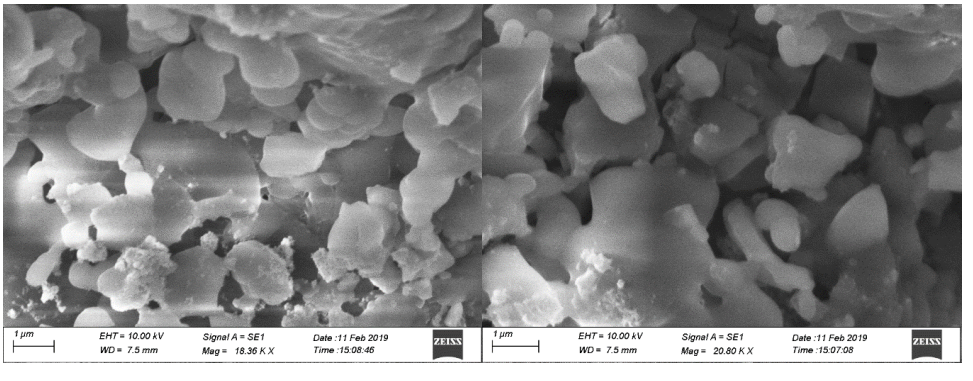

Fig. 2. SEM image of NiO nanoparticles.

3.2. *SEM analysis of NiO nanomaterial*

From the Scanning Electron Microscopy Images in Fig. 2, a flower structure was found, which was in good agreement with XRD results. Agglomeration with irregular shapes could be controlled by optimizing the reaction conditions like temperature, concentration, reducing agent and pH.

3.3. *Fourier-transform analysis of infrared spectroscopy of NiO nanomaterials*

By using FTIR spectroscopy method, one can acquire the infrared emission and absorption spectra of a solid, liquid or gas. High-spectral-resolution data are simultaneously gathered over a broad spectral range using an FTIR spectrometer. Compared to a diffusional spectrometer, which can only detect intensity over a restricted

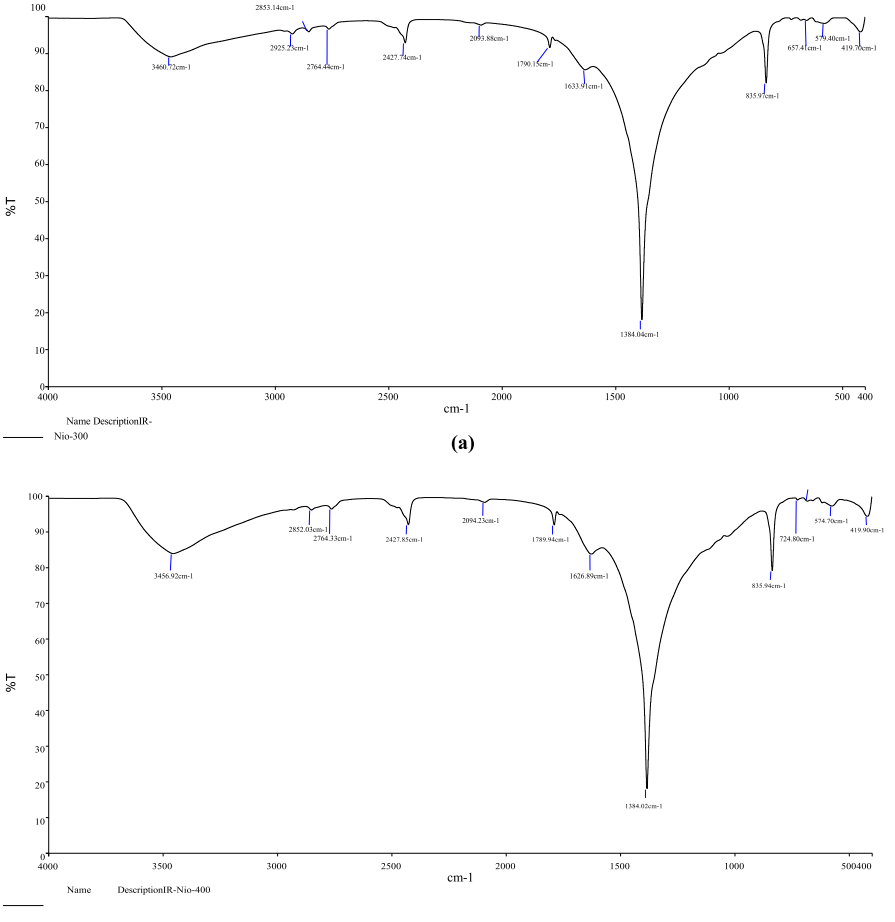

Fig. 3. (Color online) (a) NiO 300°C. (b) NiO 400°C.

range of wavelengths at once, this provides it a significant advantage. To clarify the molecular structure of the synthesized molecule, the functional groups were identified using FTIR spectroscopy. And by using a spectrum KXI spectrometer and the KB replete method at 300 K, FTIR spectra were acquired in the 400–4000 cm^{-1} region. In the NiO FTIR spectrum in Figs. 3(a) and 3(b), stretching can be seen between the ranges of 3460.72 to 1633.91 cm^{-1}. Here, the strong band at 419.70 for (300°C) and 419.90 cm^{-1} (400°C), is connected to the NiO band stretching vibration. The presence of amounts of water in the sample is indicated by the broad absorption band centered at 3450 cm^{-1}, which is attributed to O–H stretching vibrations, and the band at 1630 cm^{-1}, which is attributed to H–O–H bending vibration mode. Ni-O stretching vibration frequency is positioned in the 430–490 cm^{-1} wide absorption band. The broadness of the band indicates the nanocrystalline nature of the materials. The broad absorption band centered at 3460.72 cm^{-1} (300°C) and 3456.92 cm^{-1} (400°C) is attributed to the band O–H stretching vibrations, and the band at 1633.91 cm^{-1} (300°C) and 1626.89 cm^{-1} (400°C) is attributed to bending mode (H–O–H). The band at 1384.04 cm^{-1} (300°C) and 1384.02 cm^{-1} (400°C) is primarily due to the bending vibration of ionic CO_3^{2-}. The three bands appearing around 835.97, 657.41 cm^{-1} (300°C) and 835.94, 724.80 cm^{-1} (400°C) confirm the presence of C–O. The band at 2925.23 cm^{-1} (300°C) and 2852.03 cm^{-1} (400°C) and the band at 1384.04 cm^{-1} (300°C) and 1384.02 cm^{-1} (400°C) in Figs. 3(a) and 3(b) are because the calcined powder tends to physically absorb water and carbonate ion.[12,16,17]

4. Optical Studies

4.1. *UV–Vis spectroscopy*

From the UV–Vis spectroscopy in Figs. 4(a) and 4(b), optical absorption spectrum was obtained in the range 300–1100 nm. Absorption peak occurred at 300 nm for 300°C and 305 nm for 400°C. The electronic transition between the valence and conduction bands band is what causes these peaks.[18–20] Using the Tauc relation, the direct band energy gap was determined and is shown as follows.

$$\alpha h\upsilon = A(h\upsilon - E_g)^n, \tag{4}$$

where A is a constant, Eg is the optical energy band gap, is the heat capacity and n is a transition-dependent exponent in this work, NiO's optical band gap is at 3.37 eV (300°C) and 2.7 eV (400°C). This effect is caused by chemical vacancies or flaws in the intergranular areas, which provide new energy levels to raise the band structure energy.[20–22] From the estimated optical band gap of the nano NiO and the shift in the band gap between the bulk and the nanoparticles.[23]

4.2. *PL study*

The deep trap in Fig. 5(a) is attributed to the recombination of holes imprisoned at the inner nickel vacancies acceptor level with electrons at the internal Sulphur

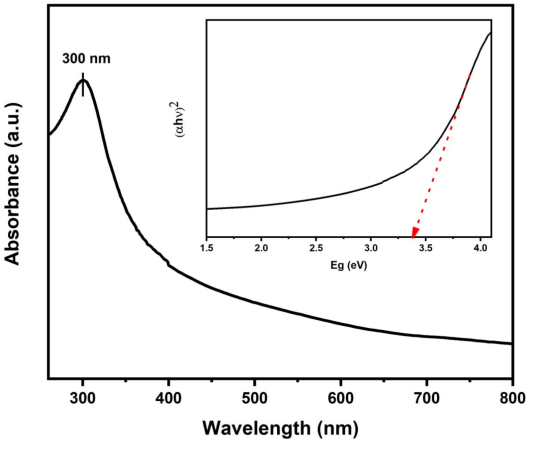

(a)

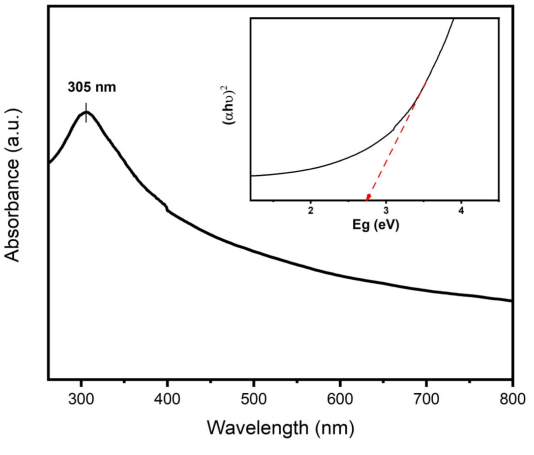

(b)

Fig. 4. (Color online) (a) UV–Vis spectrum with Tauc plot in the inserted graph for 300°C. (b) UV–Vis spectrum with Tauc plot in the inserted graph for 400°C.

vacancy donor level. To decrease the defect processes dominating the optical properties, researchers modify the surfaces of NiO nanoparticles with improved crystalline perfection by using an organic or inorganic shell.

Figure 5(b) illustrates the broad emission spectra at about 608 nm for the PL spectrum of spherical nanocrystals.

In addition, the resulting emission spectrum shows three shoulder emission peaks observed near 343, 363 and 479 nm. The other shoulder emission peaks might be attributed to near band-to-band transition and oxygen-related defects at annealing temperatures.[13,23–26]

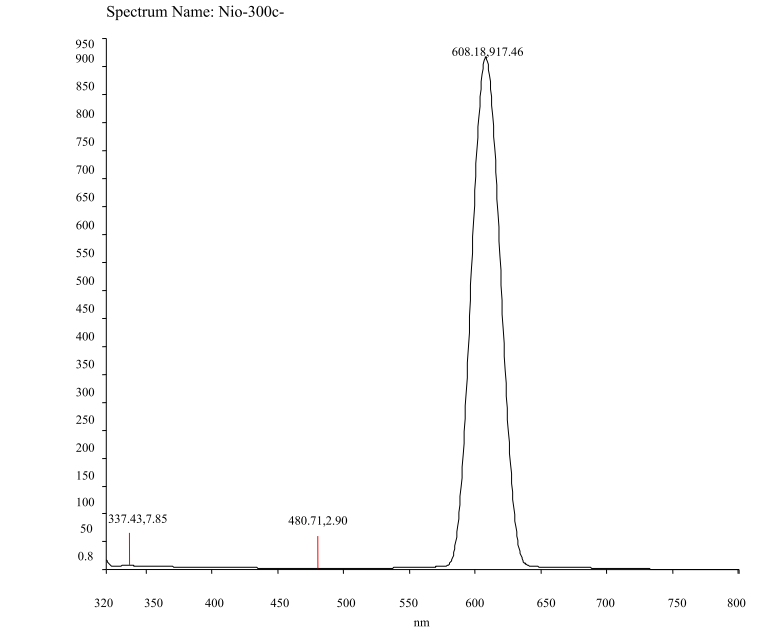

Fig. 5. (Color online) (a) PL spectrum of NiO 300°C, (b) PL spectrum of NiO 400°C.

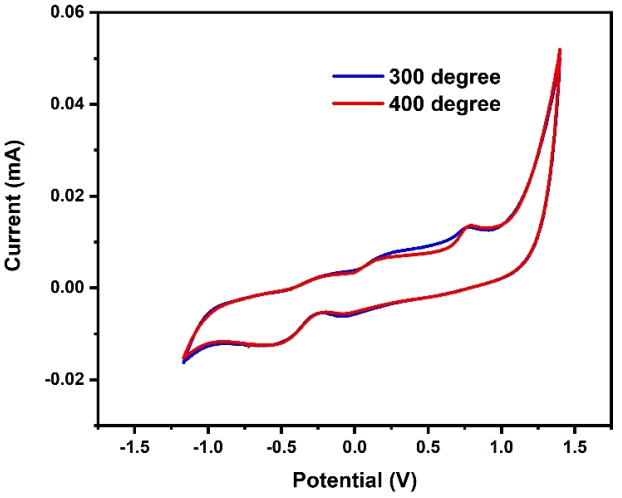

Fig. 6. (Color online) CV profile of NiO 300°C and 400°C.

5. Electrochemical Measurements

From the cyclic voltammetry (CV) graph of Fig. 6 for both the samples annealed at 300°C and 400°C, an irregular quasi-rectangular shape was observed and 2.5 V was identified to be the potential window. Minor deviation from rectangular shape is due to the predominant pseudo capacitance behavior along with the double layer charge storage mechanism. Using the formula to calculate a specific capacitance

$$\text{Csp} = \frac{\int IdV}{s \times m \times \Delta V} \text{ (F/g)}, \tag{5}$$

$\int IdV$ indicates the area beneath the curve, s denotes the scan speed, m is the substance's active mass and V is the potential window. For the sample annealing at 300°C, the specific capacitance was 543.6 F/g, while for the sample annealing at 400°C, the specific capacitance was 519.8 F/g.

6. Conclusion

Sharp and strong Bragg peaks are observed at 2θ — 37.60, 43.60, 63.20, 75.80, 79.80 corresponding to (111), (200), (220), (311), (222) plane of the cubic structure having Fm3/m space group. Scanning electron microscope (SEM) image shows the flower-like structure. Functional groups were identified using FTIR. The broad absorption band centered at 3460.72 cm^{-1} (300°C) and 3456.92 cm^{-1} (400°C) is attributed to the band O–H stretching vibrations. The strong band at 419.70 for (300°C) and 419.90 cm^{-1} (400°C), are connected to the NiO band stretching vibration. Absorption peak occurred at 300 nm for 300°C and 305 nm for 400°C and NiO's optical band gap is at 3.37 eV (300°C) and 2.7 eV (400°C). The PL Spectrum of calcinated NiO represents the nanocrystals, it shows the broad emission spectra

at around 608 nm, respectively. The electrochemical analysis of CV represents a rectangular shape, it is also similar to an electric double-layer capacitor (EDLC). The NiO nanoparticles successfully produced at 300°C and 400°C were promising materials, the specific capacitance was 543.6 and 519.8 F/g. The produced NiO nanoparticles are well-suited for supercapacitor energy storage applications.

References

1. M. Tadic, D. Nikolic, M. Panjan and G. R. Blake, *J. Alloys Compd.* **647** (2015) 1061.
2. S. M. Hussain, A. K. Javorina, A. M. Schrandss, H. M. Duhart, S. F. Ali and J. J. Schlager, *Toxicol. Sci.* (2006) 92456.
3. N. Singh, J. M. Singelyn, J. A. DeQuach, S. B. Seif-Naraghi, R. B. Littlefield, P. J. Schup-Magoffin and K. L. Christman, *Biomaterials* (2009) 303891.
4. G. Oberdörster, *Int. Arch. Occup. Environ. Health* (2000) 741.
5. M. Li, S. Pokhrel, X. Jin, L. Mädler, R. Damoiseaux and E. M. V. Hoek, *Environ. Sci. Technol.* (2011) 45755.
6. B. D. Ngom, T. Mpahane, E. Manikandan and M. Maaza, *J. Alloys Compd.* **656** (2016) 758.
7. N. L. Rosi and C. A. Mirkin, *Chem. Rev.* (2005) 1051547.
8. J. K. Dunnick, J. M. Benson, C. H. Hobbs, F. F. Hahn, Y. S. Cheng and A. F. Edison, *Toxicology* (1988) 50145.
9. M. Maaza, D. Hamidi, A. Simo, T. Kerdja, A. K. Chaudhary and J. B. Kana, *Opt. Commun.* **285** (2012) 1190.
10. M. El-Kemary, N. Nagy and I. El-Mehasseb, *Mater. Sci. Semicond. Process.* **16** (2013) 1747.
11. Y. B. M. Mahaleh, S. K. Sadrnezhaad and D. Hosseini, *J. Nanomater.* (2008) 1.
12. M. N. Siddique, A. Ahmed, T. Ali and P. Tripathi, *AIP Conf. Proc.* (1953) 030027.
13. F. T. Thema, E. Manikandan, A. Gurib-Fakim and M. Maaza, *J. Alloys Compd.* **657** (2015) 655.
14. A. T. Khalil, M. Ovais, I. Ullah, M. Ali, Z. K. Shinwari, D. Hassan and M. Maaza, *Artif. Cells Nanomed. Biotechnol.* **46** (2018) 838.
15. K. Kaviyarasu, E. Manikandan, J. Kennedy, M. Jayachandran, R. Ladchumananandasiivam, U. U. De Gomes and M. Maaza, *Ceram. Int.* **42** (2016) 8385.
16. T. Ç. Taşdemirci, *Chem. Phys. Lett.* **738** (2020) 136884.
17. G. T. Anand, R. Nithiyavathia, R. Ramesha, S. J. Sundarama and K. Kaviyarasu, *Surf. Interfaces* **18** (2020) 100460.
18. K. C. Suresh and A. Balamurugan, *Inorg. Nano-Met. Chem.* (2020) 296.
19. K. Kannagi, K. K. Purushothaman, P. Suganya and B. Sethuraman, *AIP Conf. Proc.* (2002) 2270110041.
20. V. Kumar, H. C. Swart, M. Gohain, V. Kumar, S. Som, B. C. B. Bezuindenhoudt and O. M. Ntwaeaborwa, *Chem. Eng. J.* (2014) 255541.
21. H. Yamamoto and S. Tanaka, *J. Appl. Phys.* **93** (2003) 4158.
22. L. Soriano, L. Soriano, A. Gutiérrez, I. Preda, S. Palacín, J. M. Sanz, M. Abbate, J. F. Trigo, A. Vollmer and P. R. Bressler, *Phys. Rev. B* **74** (2006) 193402.
23. M. N. Rifaya, T. Theivasanthi and M. Alagar, *Nanosci. Nanotechnol.* **2** (2012) 134.
24. D. Hassan, A. T. Khalil, J. Saleem, A. Diallo, S. Khamlich, Z. K. Shinwari and M. Maaza, *Artif. Cells Nanomed. Biotechnol.* **46** (2018) 693.
25. A. Ezhilarasi, J. J. Vijaya, K. Kaviyarasu, M. Maaza, A. Ayeshamariam and L. J. Kennedy, *J. Photochem. Photobiol. B*: *Biol.* **164** (2016) 352.
26. B. T. Sone, X. G. Fuku and M. Maaza, *Int. J. Electrochem. Sci.* **11** (2016) 8204.